Master's Thesis

Title

Dynamic Wavelength Allocation Methods in WDM-based

Optical Path/Packet Integrated Networks

Supervisor

Professor Masayuki Murata

Author

Norimitsu Tsutsui

February 15th, 2010

Department of Information Networking

Graduate School of Information Science and Technology

Osaka University

Master's Thesis

Dynamic Wavelength Allocation Methods in WDM-based

Optical Path/Packet Integrated Networks

Norimitsu Tsutsui

Abstract

Wavelength Division Multiplexing (WDM) technology multiplexes optical signals that take different wavelengths into the optical fiber, and offers a high bandwidth transmission. As an application of the WDM technology to the Internet, several network architectures have been discussed; packet-based architecture such as IP over WDM and path-based architecture that establishes a lightpath between nodes on-demand basis. In this paper, we investigate a path/packet integrated architecture for WDM-based optical networks. The main advantage of the path/packet integration is to enjoy strengths of both packet switching paradigm and circuit switching paradigm. We evaluate the performance of path/packet integrated networks via computer simulations with respect to the latency, which is defined from when a data transfer request arises to when the data transfer completes. The results show that the minimum latency depends on the amount of wavelength resources allocated to path-based network and packet-based network. We therefore develop for dynamic wavelength allocation to the networks. The threshold-based wavelength allocation method that determines the amount of wavelength resources based on the queue length of buffers in packet-based networks. We also develop the biologically-inspired wavelength allocation method based on a biological symbiosis model. The biological symbiosis model is the mathmatical model that explains co-existing and co-working of two types of bacterial strains. Simulation results show dynamic wavelength allocation methods reduce the latency more than 50% from the fixed wavelength allocation. The results also show that biologically-inspired wavelength allocation method achieves a nealy 40% reduction of the latency from threshold-based wavelength allocation method.

Keywords

Path/Packet Integration

IP over WDM

Wavelength Routing

Biological Symbiosis Model

Transmission Control Protocol (TCP)

Latency

Contents

List of Figures

List of Tables

1 Introduction

New services such as cloud computing, P2P file sharing, and CDNs (Contents Delivery Networks) will drive the traffic growth and bandwidth demands in the future [1]. The answer to meet the bandwidth demand is centered on a new emerging technology, WDM (Wavelength Division Multiplexing). WDM technology allows transmitting multiple optical signals on different wavelengths on a single fiber, which dramatically increases the link bandwidth. However, increasing the link bandwidth by WDM technology does not resolve the network bottleneck sufficiently because of the limitation of packet processing capacity of routers.

In recent years, advances in optical technologies have led to WDM technology with networking capabilities. One of important features to overcome the limitation of packet processing capacity of routers is a wavelength-routing capability at the optical layer. That is, optical-signal is routed via OXCs (Optical Cross Connects) in WDM-based network, and a wavelength channel, which is also known as lightpath, is prepared between two electronic nodes. In this case, no electronic processing is necessary inside the WDM-based network.

To effectively utilizing the wavelength-routing capability, two approaches have been investigated in the literatures [2, 3]. One of approaches is to transfer the data based on the circuit-switching paradigm. That is, when a data transfer request arises at a source node, a wavelength is dynamically reserved between the source and destination nodes and a lightpath is configured. Then, the data is transferred using the allocated wavelength channel. After the data transmission using the lightpath, the lightpath is immediately torn down (i.e., the wavelength is released). The main strength of the circuit-switching paradigm is the data request solely uses and enjoys the bandwidth of wavelength channels, which would be attractive for recent multimedia services and/or cloud services that require high reliability and large bandwidth. Another strength is that a congestion avoidance mechanism is no longer necessary. That is, any transport protocols other than TCP can be used for the data transfer. In a recent study, a transport protocol that effectively utilizes the wavelength channel is investigated in Ref. [4]. The drawbacks of this approach are the lightpath setup delay, defined from when data transfer request arises to time when data transfer starts, and blocking during the lightpath establishment. Another approach is called IP-over-WDM [5, 6] where a data is transferred based on packet switching paradigm. In this approach, each node consists of IP router and OXC (Optical Cross Connect) that binds an input wavelength channel to a

6

specified output wavelength channel. Then, a virtual network topology (VNT) is constructed in advance by setting up lightpaths between two IP routers. The lightpath behaves as the virtual link from viewpoint of IP networks. That is, a data transfer is performed based on the packet switching paradigm over the VNT.

The current Internet is mainly based on the packet switching paradigm. However, many problems arise with increasing traffic demand and advances of related networking technologies and networking services. For example, the packet drop rate and packet delay increases because of congestion caused by other user traffic [7], which is an inevitable characteristic and may be crucial for services requiring high reliability and large bandwidth. To relax this, over-provisioning of link capacity and router's processing capability are widely used. However, the over-provisioning is eventually difficult because of technological constraints, such as the limitation of packet processing speeds, and economical constraints, such as power-consumption for high-speed (but high-cost) packet processing interfaces. Although more advances of technology may resolve the limitation of packet processing capacity and reduce the cost, the above-mentioned characteristics are essential for the packet-switching paradigm.

Both the circuit switching paradigm and the packet switching paradigm have streangths and weaknesses. Therefore, constructing only packet switched network or circuit switched network cannot satisfy requirements, such as the high reliability and large bandwidth, for future networking services. Thus, an integration of circuit switched network and packet switched network is required to enjoy strength of both circuit-switching paradigm and packet-switching paradigm. One possible approach to fulfill this is to deploy the WDM technology and allocate different wavelengths for each network. Hereafter, we will call a network based on the packet-switching paradigm as the packet-based network and call a network based on the circuit-switching paradigm as the path-based network.

In this thesis, we investigate the performance of path/packet integrated networks. Here, the integration is made by allocating a part of wavelengths to the packet-based network and the rest of wavelengths to the path-based network. Reference [8] also evaluates the performance of path/packet integrated networks with respected to the network throughput. The results reveal that the path/packet integrated network actually increases the network throughput. However, as we will see in Section 4, the results also reveal that the optimal wavelength allocation depends on the arrival rate of data transfer requests. We therefore develop dynamic wavelength allocation meth-

7

ods that dynamically reconfigure the number of allocated wavelengths for achieving minimum latency on the current network environments. We propose two dynamic wavelength allocation methods: the one is based on a threshold of queue length of buffer in packet-based network and the other is based on a biological symbiosis model developed in [9]. We first evaluate the latency via computer simulations with fixed wavelength allocation that allocates a pre-specified number of wavelengths to each network. Numerical results show that the path/packet integrated network actually decreases the latency. The results also show the optimal number of wavelengths allocated to path/packet integrated networks depends on traffic load. We then evaluate our two dynamic wavelength allocation methods and compare them with the fixed wavelength allocation. Our results show that the latency with dynamic wavelength allocation methods is decreased even when traffic load is changed.

This thesis is organized as follows. In Section 2, we introduce the network architecture of path/packet integrated networks. In Section 3, we evaluate the performance of path/packet integrated networks with the fixed wavelength allocation. In Section 4, we explain two dynamic wavelength allocation methods and evaluate their performance in path/packet integrated networks. Section 5 concludes this thesis.
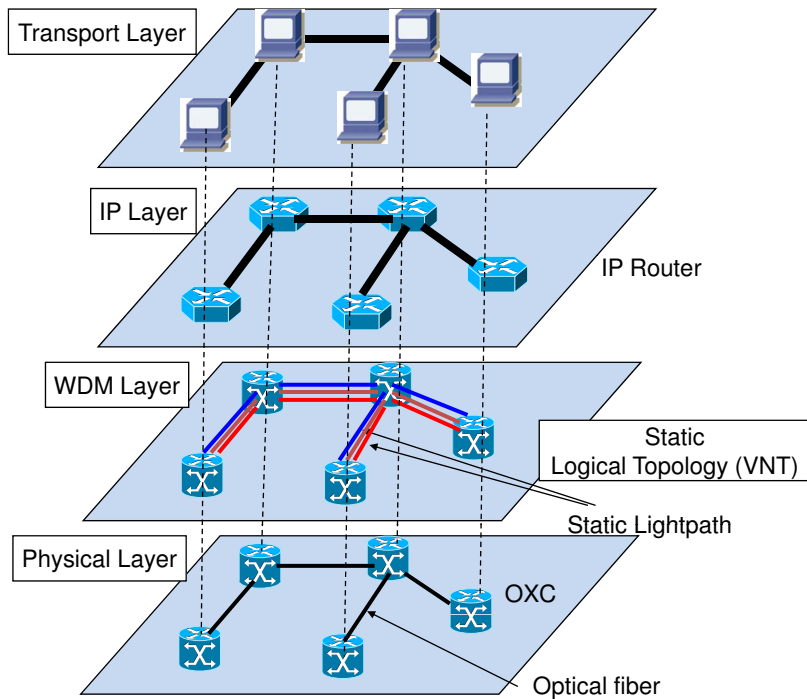
Figure 1: Packet switching over WDM networks

2 Optical Path/Packet Integrated Architecture

2.1 Packet switching over WDM networks

One of approaches that effectively utilize the wavelength-routing capability is IP-over-WDM [5,6] where a virtual network topology is constructed on top of the physical topology. In this approach, each node consists of IP router and OXC (Optical Cross Connect) that binds an input wavelength channel to a specified output wavelength channel. Then, lightpaths are established by configuring OXCs between two IP routers (Figure 1) and behaves as the virtual link from viewpoint of IP networks. A data transfer is made based on the packet switching paradigm and therefore IP-over-WDM has good compatibility with the current Internet. Furthermore, IP-over-WDM can achieve high link utilization thanks to statistical multiplexing of packets from different connections. However, IP-over-WDM cannot provides large bandwidth to each connection because it leads to the congestion of user traffic, forwarding processing delay, and packet drop at routers.
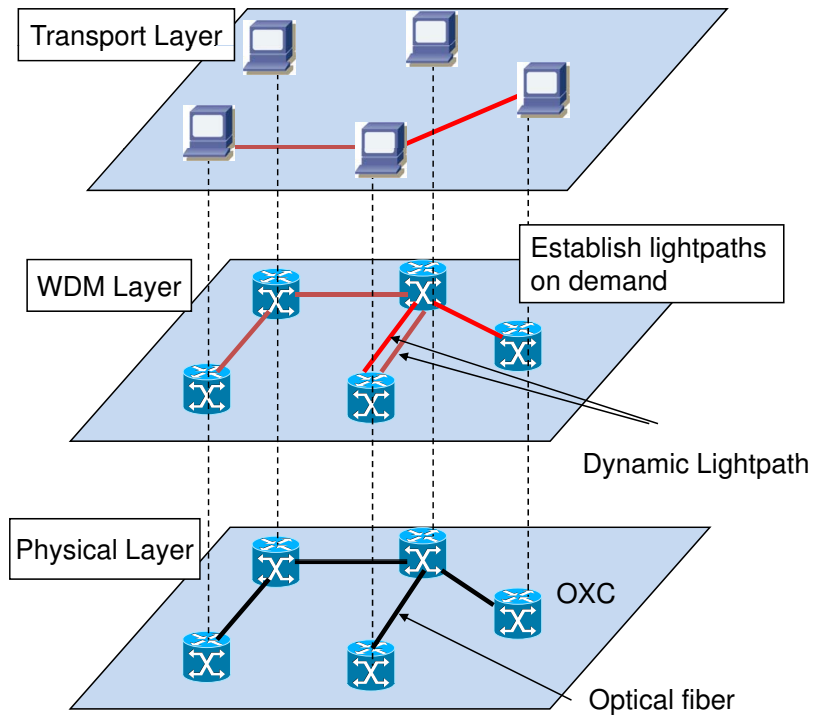
Figure 2: Path switching over WDM networks
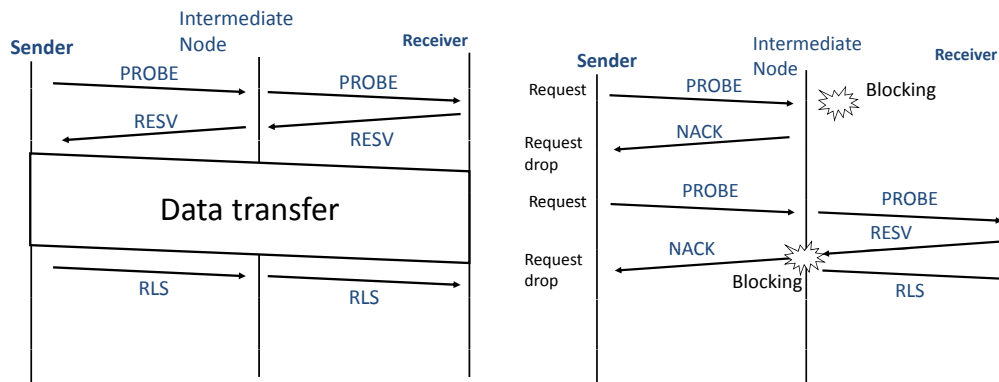
(a) Successful case

(b) Failure case

Figure 3: Backward reservation for lightpath establishment

2.2 Path switching over WDM networks

Another approach that effectively utilize the wavelength-routing capability is to transfer the data on demand basis. That is, when a data transfer request arises, lightpaths are immediately established

between source and destination nodes (Figure 2). In this thesis, we use a RSVP-based wavelength reservation protocol with a full wavelength converter. The overview of RSVP-based protocol with backward reservation method is as follows.

In backward reservation with full wavelength converter, the source node sends a PROBE packet before a wavelength reservation. A PROBE packet collects the usage of wavelengths along the forward path and does not reserve wavelengths at this time. Along the forward path, the PROBE packet checks if there is any available wavelengths or not in the next link and sends the packet toward destination node. When the destination node receives a PROBE packet, the information in the PROBE packet is retrieved and check whether there is one more available wavelengths between the source and destination or not. Based on the information, the destination node determines a wavelength for reservation, and then sends a RESV packet toward the source node. Figure 3(a) shows when the wavelength reservation succeeds and a lightpath is established between source and destination nodes. There are two cases for the lightpath establishment. The first case is the PROBE-failure when an intermediate node or a source node knows that no wavelength is available on a link between source and destination nodes. In this case, the node returns a NACK packet toward the source node and the source node notice that the lightpath establishment fails. The second case is caused by the wavelength reservation failure on the backward path. Because of the propagation delay, the information collected by a PROBE packet may be different from the link state at when the RESV packet arrives. Figure 3(b) shows the case when the wavelength reservation during the backward path fails.

When the lightpath is established between source and destination nodes, the source node can use the bandwidth of the lightpath with no congestion and packet drop since the lightpath is dedicated channel for the connection, which can be used for high reliable and large bandwidth applications. However, there is a disadvantage for this approach; A data transfer cannot start immediately when the request arises because of lightpath setup delay of propagation delay for RSVP signaling and OXC configuration delay.

(a) The case when the path switching plane   (b) The case when the packet switching plane
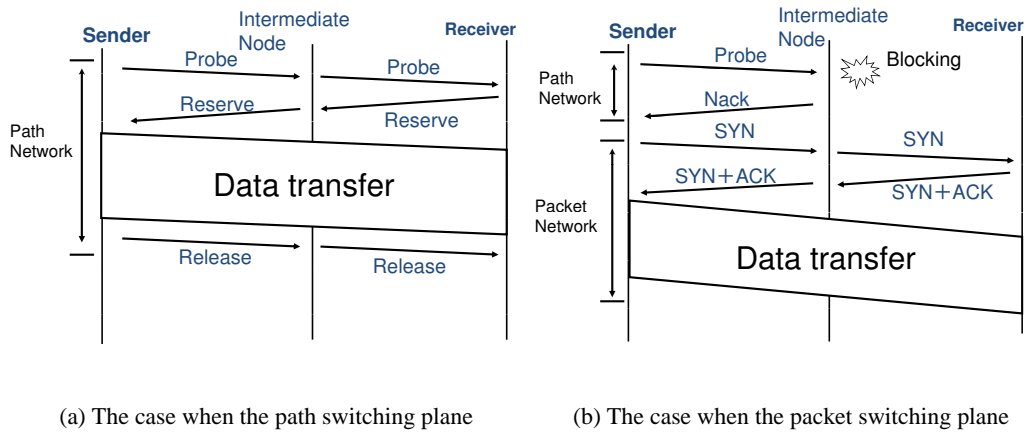
Figure 4: Control messages exchanged for a data transfer in path/packet integrated networks

2.3 Integration of optical path and packet switching

Each node in path/packet integrated networks consists of IP router and OXC. OXCs are connected with optical fiber. The path/packet integrated networks provides a packet switching plane, which works for packet-based network, and a path switching plane, which works for path-based network, by allocating wavelengths for each plane. Each end-host connecting with the node has two network interfaces; one for forwarding IP packet via packet switching plane and one for establishing a lightpath between two end-hosts. When the data transfer request arises, the end-host selects the packet switching plane or the path switching plane to transfer the data. Various strategies to select the plane can be considered. The optimal strategy highly depends on the traffic characteristics, so instead of developing the sophisticated strategy, we take a simple strategy to select the plane because our primary concern of the current paper is to show whether the path/packet integrated networks lowers the latency or not.

Our simple strategy to select the plane is as follows. When the data transfer request arises, the sender host first tries to transfer the data in path switching plane. After the lightpath establishment succeeds, the sender host transfers the data with the bandwidth of the lightpath. When the lightpath establishment fails, the sender host gives up transferring the data via the path switching plane, and transfers the data via the packet switching plane. In this case, the sender host uses the TCP protocol for the data transfer. Figure 4 illustrates control messages exchanged during a data transfer.

(a) The case when λ_1 is used for path switching plane

(b) The case when λ_1 is used for packet switching plane
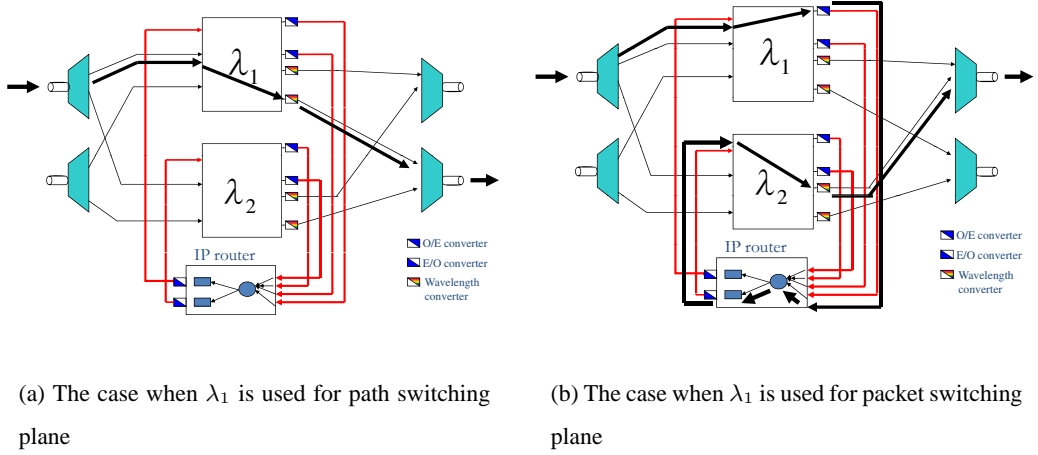
Figure 5: A node architecture for fixed wavelength allocation

3 Latency Evaluation of Path/Packet Integrated Networks with Fixed Wavelength Allocation

3.1 Node architecture for fixed wavelength allocation

In this section, we present a node architecture for fixed wavelength allocation. Figure 5 depicts the node architecture where two wavelengths (denote λ_1 and λ_2) are multiplexed on a link. When λ_1 is allocated to the path switching plane (Figure 5(a)), packets on lightpaths are not processed by the IP router. Thus, the incoming optical-signal is directly forwared to the output port. When λ_1 is allocated to the packet switching plane (Figure 5(b)), each packet arriving at λ_1 in input ports is converted from the optical signal to an electronic signal, and is directed to the IP router. The packet is then processed by the IP router for routing, and then stored in the buffer prepared for each output port. The packet is again converted from the electronic signal to optical signal and is forwarded to the output port. Note that we can consider various kinds of node architectures. Our node architecture used in this paper requires lots of input and output ports for IP router and OXCs. Further investigation is necessary to reduce the nodal costs.

3.2 Simulation Parameters

For our evaluation, we use the dumbbell network shown in Figure 6. The network has sender hosts and receiver hosts equipped with two network interfaces. Nodes, each having IP router and OXC,
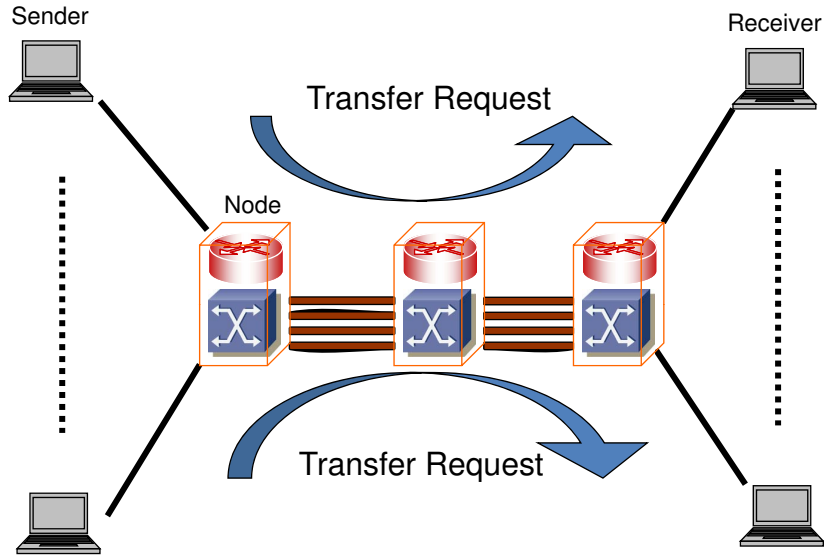
Figure 6: Dumbbell network

Table 1: Simulation parameters

Topology	Dumbbell
OD pairs	120
OXC configuration delay	0 ms
Link propagation delay	10 ms
Arrival process	Poisson
Amount of data	Exponential distribution with mean 1 Gbit
Bandwidth of a wavelength	10 Gbps
Number of wavelengths	8
Buffer size at IP routers	256 MB

are connected with hosts via the network interfaces, and are also connected with each other via WDM transmission link. The number of wavelengths multiplexed between nodes is eight, and the buffer size of each IP router is 256MB. In this evaluation, we assume that the bandwidth of links between sender hosts and nodes is enough not to be a bottleneck of path/packet integrated networks.

In the packet switching plane, the packet is processed based on the FIFO (First-in First-out) drop-tail discipline. The sender host employs TCP Reno when the data is transferred via the packet switching plane. When the path switching plane is used, the sender host transfers the data with the maximum bandwidth of wavelengths since the sender host exclusively uses the lightpath. The other simulation parameters are summarized in Table 1 .

The performance metric used in this paper is the average latency. We define latency as the time from when a data transfer request arises to when the data transfer completes. The formal definition of the average latency is,

$$(\sum_{i=1}^{n_c} P_i + \sum_{k=1}^{n_p} B_k + \sum_{k=1}^{n_p} T_k)/(n_c + n_p), \tag{1}$$

where n_c is the number of data transfers completed by using the path switching plane and n_p is the number of data transfers completed by using the packet switching plane. P_i represents the latency of the i-th request among the n_c requests. For the k-th request among the n_p requests, we define B_k as the time consumed for exchanging the control messages to establish a lightpath and define T_k as the time from when a TCP session starts to when the data transfer completes.

3.3   Simulation results and discussions

An average latency of path/packet integrated networks is shown in Figure 7. In the figure, the x-axis represents the number of wavelengths allocated to the path switching plane. The WDM link has eight wavelengths, so the rest of wavelengths are used for the packet switching plane. Note that we statically allocate wavelengths resources to the path/packet switched networks in the current evaluation. We show the average latency when the arrival rates of data transfer request at bottleneck link are 9.6 requests/s ("LowLoad" in the figure), and 28.8 requests/s ("HighLoad" in the figure). In the case of "LowLoad", the latency decreases as the number of wavelengths allocated to the path switching plane increases. This is because more requests are accommodated in the path switching plane. In the case of "HighLoad", the lowest average latency is achieved when the number of wavelengths allocated to the path switching plane is five or six wavelengths. The reason is as follows. The latency of the path switching plane eventually decreases as the number of wavelengths allocated to the path switching plane increases. However, as the number of wavelengths allocated to the path switching plane increases, the bandwidth allocated for the packet switching plane becomes narrow, which leads to the increase of the average latency. That
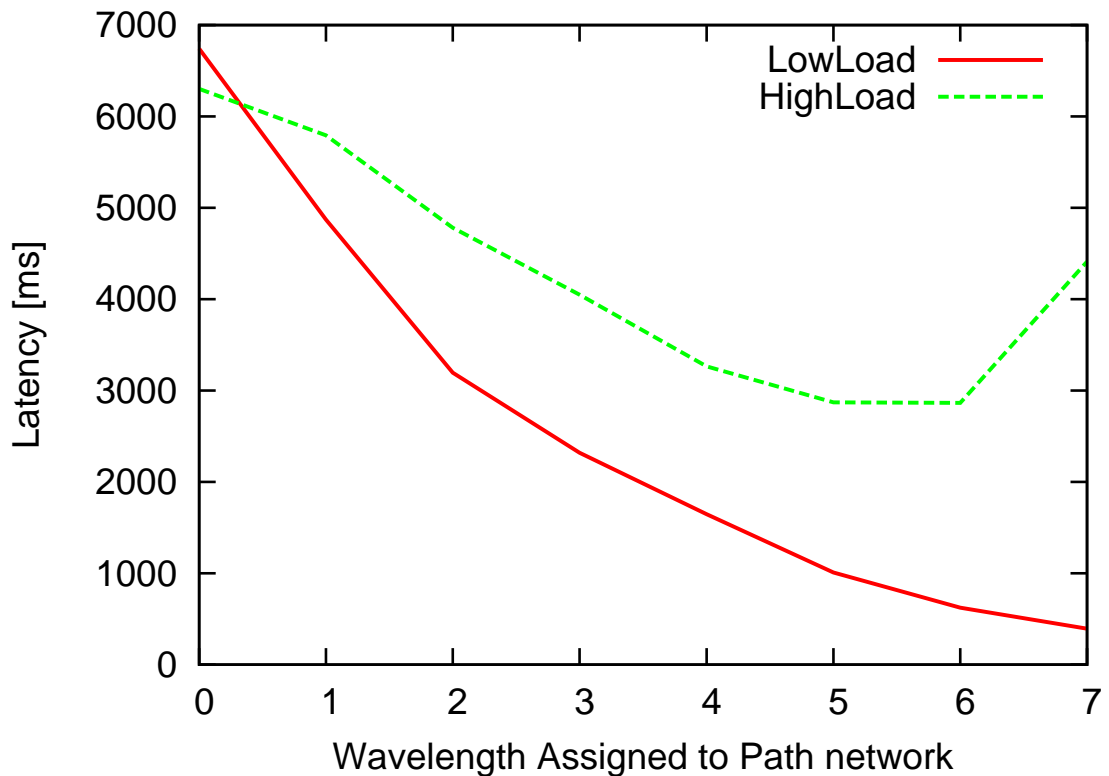
Figure 7: Average latency of path/packet integrated networks

is, an optimal number of wavelengths allocated to each network depends the traffic load and traffic characteristics.

We next show the average latency of path/packet integrated networks when the buffer size of routers are changed. Figure 8 show the average latency depends on the number of wavelengths allocated to the path switching plane. The arrival rate of data transfer request at the bottleneck link is set to 38.4 requests/s. In the figure, we show the results when the buffer sizes of routers are 4MB, 16MB, and 64MB. We observe that the latency of path/packet integrated networks decreases to around 25% of the latency in the packet switching plane. That is, the path/packet integrated networks is effective with regard to the reduction of buffer size in the router. Note that we can see the latency in the packet switching plane by looking at the value when x-axis is 0 in Figure 8. The minimum latency is achieved when the buffer size is small due to the lower queuing delay in the buffer.

16
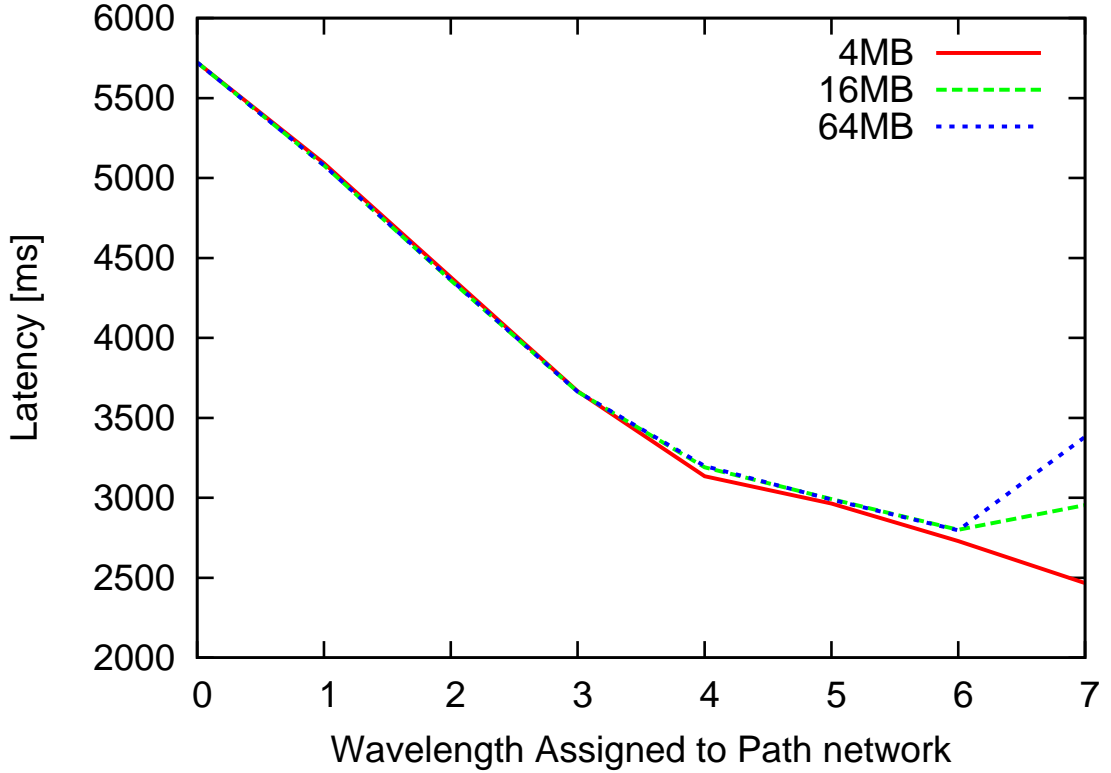
Figure 8: Effects of buffer size on latency

4 Dynamic Wavelength Allocation Methods in Optical Path/Packet Integrated Networks

4.1 Enabling node architecture

We first show the node architecture that enables dynamic wavelength allocation. The architecture is almost the same the architecture shown in Figure 9. The difference is that there is a controller to manage the configuration of OXCs and observe the network environment, such as the buffer utilization of IP routers, the blocking rate of lightpath establishments, and the packet dropped rate in the IP router. Depending on the wavelength methods explained in later, the controller collects the buffer utilization of IP router (in threshold-base wavelength allocation) or the blocking rate and the packet drop rate in the IP router (in biologically-inspired wavelength allocation). Figure 9 shows the node architecture that multiplexes four wavelengths on a link. In Figure 9(a), two wavelengths (λ_1 and λ_2) are assigned to the path switching plane, and the other two wavelengths (λ_3 and λ_4) are assigned to the path switching plane. When the controller determines to increase the amount

(a) Two wavelengths allocated to the path switching plane

(b) Three wavelengths allocated to the packet switching plane
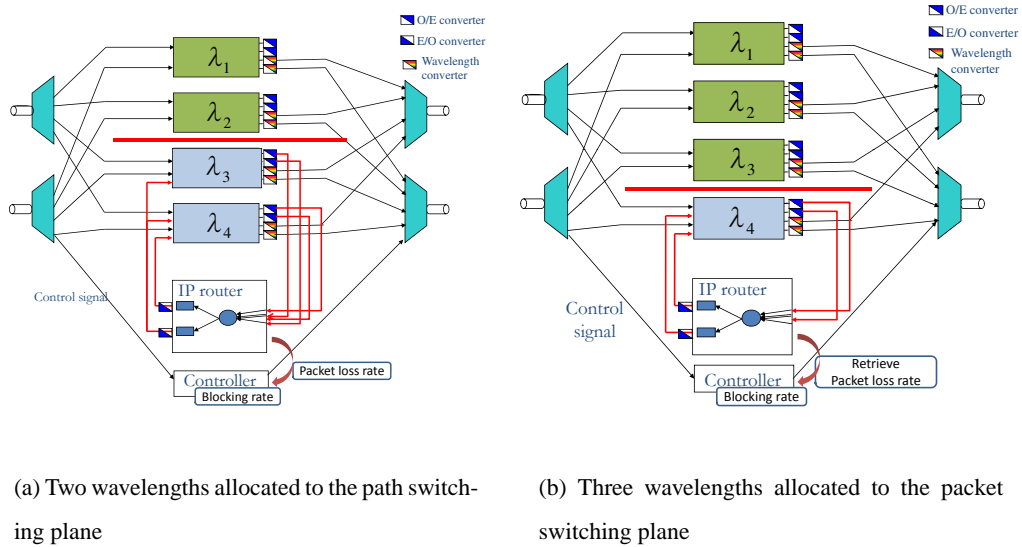
Figure 9: Node architecture for dynamic wavelength allocation

of wavelengths allocated to the path switching plane, the controller immediately reconfigure the optical switch for λ_3 so as not to forward the optical-signal to the IP router. In this way the node is configured to Figure 9(b).

4.2 Threshold-based wavelength allocation method

We first present the threshold-based wavelength allocation method for dynamic wavelength allocation. As we have seen the results of fixed wavelength allocation, relaxing the congestion of the packet switching plane is important to reduce the overall latency. To relax the congestion of the packet switching plane, we use the average queue length of IP router as the sign of redundancy / shortage of wavelength resources for the packet switching plane. When the average queue length is getting long, it means that too many packets are transferred through the packet switching plane. Therefore, the number of wavelengths allocated to the packet plane should be increased. When the average queue length is getting short or zero, it means that less congestion for the packet switching plane. In this case, the number of wavelengths allocated to the packet switching plane should be decreased to reduce the overall latency since the data transfer through the lightpath minimizes the latency. Based on this observation, we introduce the following dynamic wavelength allocation method to each outgoing link.

18

Step. 1: The controller in the node measures queue length and calculates the average queue length periodically

Step. 2: When the average queue length exceeds a maximum threshold, t_{max} , of buffer size, go to Step. 3. When the average queue length is less than a minimum threshold, t_{min} , of buffer size, go to Step 4. Otherwise go back to Step. 1

Step. 3: Increase the number of wavelengths allocated to the packet switching plane by one. Consequently, the number of wavelengths allocated to the path switching plane decreases by one. Go back to Step. 1

Step. 4: Decrease the number of wavelengths allocated to the packet switching plane by one. Consequently, the number of wavelengths allocated to the path switching plane increases by one. Go back to Step. 1

We next discuss how to decide the threshold value for our threshold-based wavelength allocation method. The threshold value effects on the amount of wavelengths allocated to the path switching plane and the packet switching plane. When the maximum threshold, t_{max}, is high, the amount of wavelength allocated to the packet switching plane is less sensitive to the increase of the queue length of the buffer. When th e minimum threshold, t_{min}, is high, the amount of wavelength allocated to the packet switching plane is sensitive to the increase of the queue length. We prepare the four scenarios for t_{max} and t_{min} and conduct computer simulations to decide the threshold values.

(1) Setting t_{max} to 60% and t_{min} to 10%

(2) Setting t_{max} to 60% and t_{min} to 30%

(3) Setting t_{max} to 80% and t_{min} to 10%

(4) Setting t_{max} to 80% and t_{min} to 30%

We set the arrival rate of data transfer request to be 10.8 request/s, and increase the arrival rate to be 32.4 requests/s during [100s - 300s] and [500s -700s]. The other parameters are the same as the case of fixed wavelength allocation (See Table 1). The simulation results are summarized in Table 2.

Table 2: Simulation results for threshold-based wavelength allocation methods

	t_{max} 60% t_{min} 10%	t_{max} 60% t_{min} 30%	t_{max} 80% t_{min} 10%	t_{max} 80% t_{min} 30%
Latency (overall)	2619 [ms]	2634 [ms]	3095 [ms]	3187 [ms]
Latency (packet switching plane)	12633 [ms]	12858 [ms]	15330 [ms]	15989 [ms]
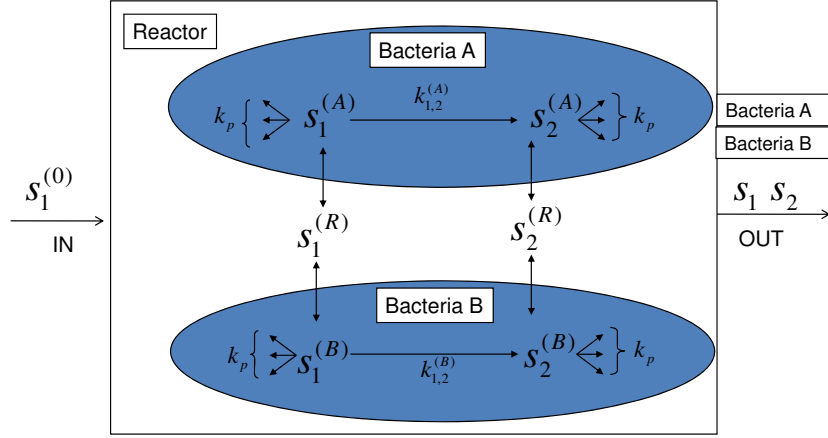
Figure 10: The biological symbiosis model

4.3 Biologically-inspired wavelength allocation method

4.3.1 Biological Symbiosis Model

In [9], the authors proposed a mathematical model of a mechanism that permitted two types of bacterial strains to live together by exchanging metabolites through a reactor. Bacterial strains have a metabolic network of generating metabolite S_2 from other metabolite S_1. Metabolites diffuse in and diffuse out of a cell through membrane depending on the difference in metabolic concentrations (Figure 10). The dynamics of concentrations of metabolites in a cell of strain A and B are formulated as,

$$ds_1^{(A)}/dt = (P/V)(s_1^{(R)} - s_1^{(A)}) - (k_{1,2}^{(A)} + k_p)s_1^{(A)}, \qquad (2)$$

$$ds_1^{(B)}/dt = (P/V)(s_1^{(R)} - s_1^{(B)}) - (k_{1,2}^{(B)} + k_p)s_1^{(B)}, \qquad (3)$$

$$ds_2^{(A)}/dt = (P/V)(s_2^{(R)} - s_2^{(A)}) + k_{1,2}^{(A)}s_1^{(A)} - k_p s_2^{(A)}, \qquad (4)$$

$$ds_2^{(B)}/dt \quad = \quad (P/V)(s_2^{(R)} - s_2^{(B)}) + k_{1,2}^{(B)}s_1^{(B)} - k_p s_2^{(B)}, \tag{5}$$

where P stands for the permeation coefficient of cell membrane, V does for the average volume of a cell. $s_{1,2}^{(A)}$, $s_{1,2}^{(B)}$ and $s_{1,2}^{(R)}$ are metabolite concentrations in a cell of strain A and B in the reactor, respectively. k_p is the metabolite consumption rate in a cell. $k_{1,2}^{(A)}$ and $k_{1,2}^{(B)}$ are the metabolite conversion rate in a cell of strain A and B. Next, metabolite concentrations in the reactor evolve as,

$$ds_1^{(R)}/dt \quad = \quad D(s_1^{(0)} - s_1^{(R)}) + X^{(A)}P(s_1^{(A)} - s_1^{(R)}) + X^{(B)}P(s_1^{(B)} - s_1^{(R)}), \tag{6}$$

$$ds_2^{(R)}/dt \quad = \quad D(s_2^{(0)} - s_2^{(R)}) + X^{(A)}P(s_2^{(A)} - s_2^{(R)}) + X^{(B)}P(s_2^{(B)} - s_2^{(R)}), \tag{7}$$

where $X^{(A)}$ and $X^{(B)}$ stand for the number of cells of strain A and B per volume in the reactor. The fresh medium containing metabolites of concentration $s_1^{(0)}$ and $s_2^{(0)}$ are added to the reactor at the constant rate and the culture is drained at the same rate. D means the resultant dilution rate. Change in population of cells is formulated as,

$$dX^{(A)}/dt \quad = \quad u^{(A)}X^{(A)} - DX^{(A)}, \tag{8}$$

$$dX^{(B)}/dt \quad = \quad u^{(B)}X^{(B)} - DX^{(B)}, \tag{9}$$

where the growth rate $u^{(A)}$ and $u^{(B)}$ is defined as,

$$u^{(A)} \quad = \quad \alpha s_1^{(A)} s_2^{(A)}, \tag{10}$$

$$u^{(B)} \quad = \quad \alpha s_1^{(B)} s_2^{(B)}, \tag{11}$$

Eq. (10) implies that a cell with high metabolite concentration grows fast. Here, $\alpha > 0$ is a constant.

4.3.2 Control approach of Biological Symbiosis Model

In this section, we explain how the biological symbiosis model can be applied to the wavelength allocation methods. More specifically, we describe how to determine the amount of wavelengths allocated for the packet switching plane and the path switching plane. Since the biological symbiosis model does not distinguish the role of A and B, we regard the bacteria A for the path switching plane and the bacteria B for the packet switching plane.

Table 3 is the correspondence table between parameters in biological symbiosis model and our wavelength allocation method. The number of bacteria A, $X^{(A)}$, represents number of wavelengths allocated to the path switching plane and the number of bacteria B, $X^{(B)}$, represents the number of wavelengths allocated to the packet switching plane. In calculating $X^{(A)}$ and $X^{(B)}$ from Equations 2-10, we need to specify definitions of $k_{1,2}^{(A)}$ and $k_{1,2}^{(B)}$ since they represent degree of productivity of the path switching plane and the packet switching plane. In our model, the degree of productivity is derived from the throughput of each plane, that is, $k_{1,2}^{(A)}$ and $k_{1,2}^{(B)}$ is calculated from following equations,

$$k_{1,2}^{(A)} = (1.0 - P_b) * C, \tag{12}$$

$$k_{1,2}^{(B)} = (s/RTT) * \sqrt{(3/2)} * \sqrt{(1/p)}, \tag{13}$$

where P_b is the blocking rate of lightpath establishments on the path switching plane and C is the bandwidth of lightpaths (in [Gbps]). B is the packet size and RTT is the propagation delay of connections. p is the packet loss probability in the packet switching plane. β is the parameter that adjusts the throughput by [Gbps] and is set to 10^{-9}. Note that $k_{1,2}^{(B)}$ is TCP's throughput calculation formula and RTT should be determined by the observed round-trip time. However, in our simulation, RTT is set to the propagation delay because the queuing delay is relatively small in the WDM-based networks. In the realistic situation, we may need the RTT estimation at the controller in nodes [10].

4.4 Simulation parameters

We again use the dumbbell topology to evaluate dynamic wavelength allocation methods. For the biologically-inspired wavelength allocation methods, we set the parameters to be $k^{(P)} = 1$, $D = 0.7$, $P = 1$, $\alpha = 1$, and $S_1^{(0)} = 8$. For the arrivals of data transfer requests, we prepare three scenarios:

(1) The arrial rate of data transfer request is set to be 13.2 request/s for [0s-100s, 900-1500s], and increase the arrival rate to be 32.4 requests/s for [100s -900s] (Figure 11(a));

(2) The arrival rate is set to be $\beta \cdot 10.1$ request/s . The β is the integer number between 1 to 5 and is selected randomly for every 100s. See Figure 11(b) for the results.

Table 3: Correspondence table between parameters in biological symbiosis model and dynamic wavelength allocation method

$X^{(A)}$	Number of wavelengths allocated to the path switching plane	$X^{(B)}$	Number of wavelengths allocated to the packet switching plane
$s_1^{(A)}$	Number of wavelengths allocated to the path switching plane per unit of time	$s_1^{(B)}$	Number of wavelengths allocated to the packet switching plane per unit of time
$s_2^{(A)}$	Throughput in the path switching plane per unit of time [Gbps]	$s_2^{(B)}$	Throughput in the packet switching plane per unit of time [Gbps]
$k_{1,2}^{(A)}$	Throughput of the path switching plane [Gbps]	$k_{1,2}^{(B)}$	Throughput of the packet switching plane [Gbps]
$u^{(A)}$	Growth rate of the path switching plane per unit of time	$u^{(B)}$	Growth rate of the packet switching plane per unit of time
$s_1^{(R)}$	Internal variable that represents the remaining wavelength resources that are not assigned to switching planes	$s_2^{(R)}$	Internal variable that represents throughput per unit of time [Gbps]
$s_1^{(0)}$	Number of wavelength multiplexed on a fiber	$s_2^{(0)}$	Parameter (set to 0)
$k^{(p)}$	Parameter	D	Parameter
P	Parameter	α	Parameter

(3) The arrival rate is set to be $\beta \cdot 15.6$ request/s . The β is the integer number between 1 to 5 and is selected randomly for every 100s.

See Figure 11(c) for the results.

For comparison purpose, we prepare the fixed wavelength allocation with seven wavelengths for the path switching plane (and thus one wavelength for the packet switching plane). In addition, we prepare the optimal wavelength allocation method by assuming that the arrival rate is known beforehand. Here, the optimal stands for achieving minimum latency with fixed wavelength allocation. In the threshold-based method, the average queue length of buffer is retrieved every 30

seconds, while the biologically-inspired wavelength allocation method is operated at every second.
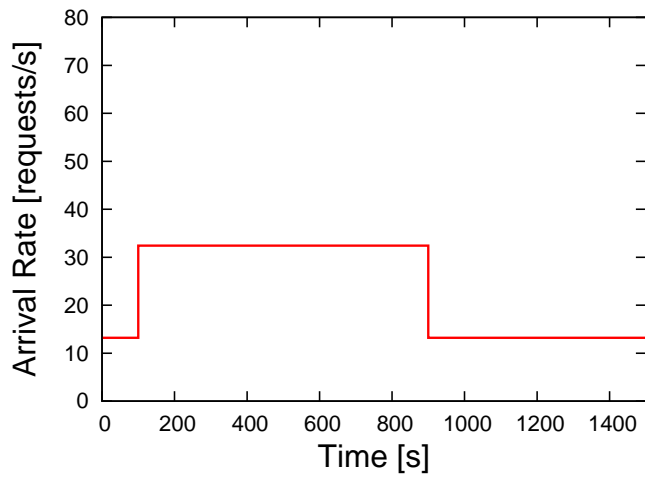
(a) Scenario 1
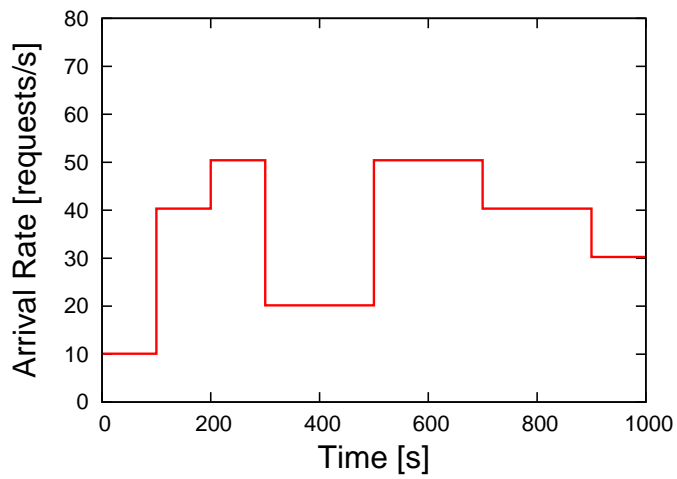
(b) Scenario 2
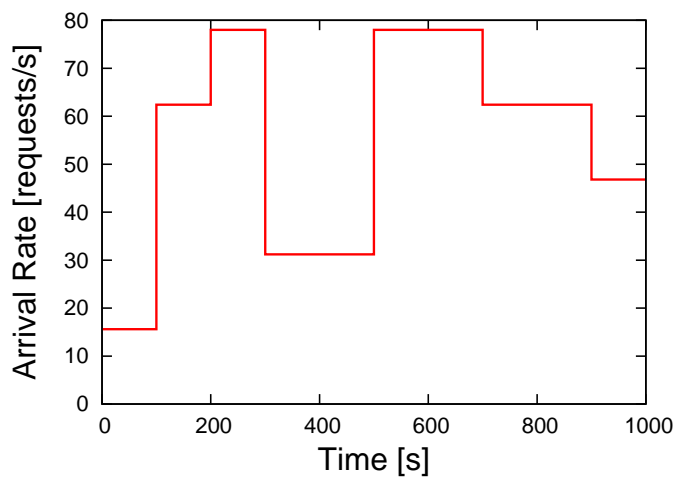
(c) Scenario 3

Figure 11: Time variation of arrival rate for three traffic scenarios

(a) Optimal wavelength allocation

(b) Fixed wavelength allocation

(c) Threshold-based wavelength allocation

(d) Biologically-inspired wavelength allocation
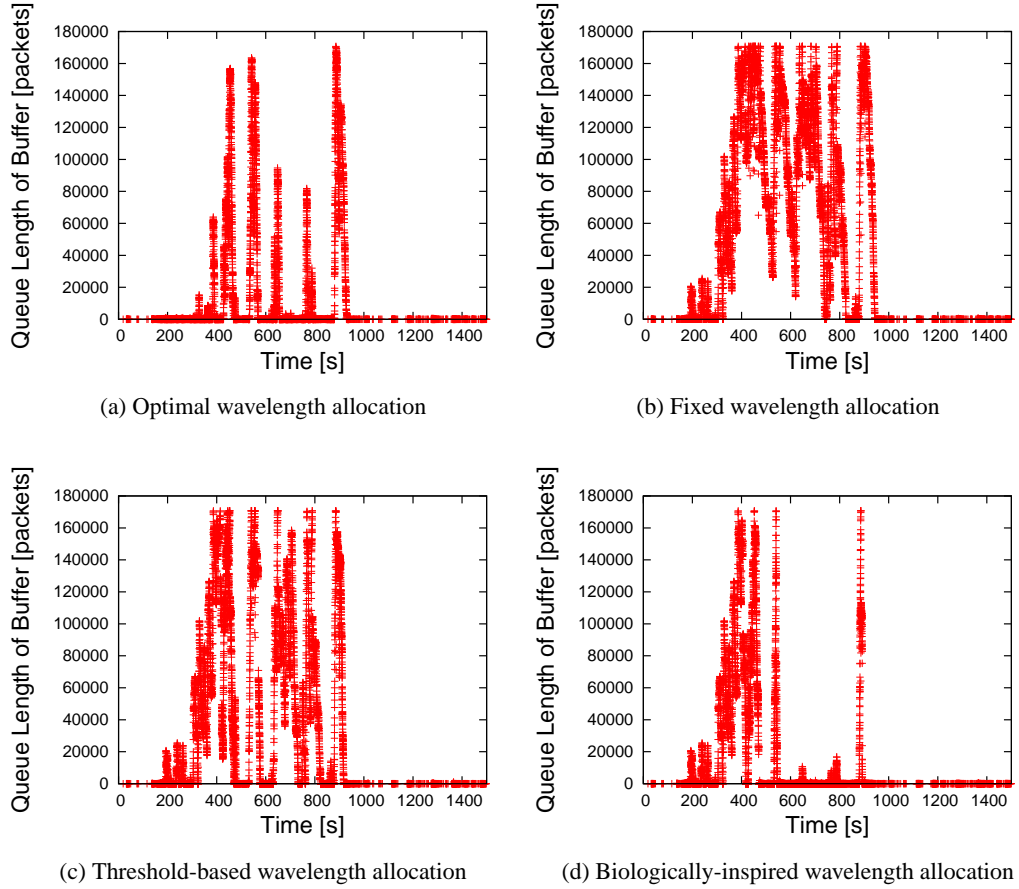
Figure 12: Time variation of queue length : Scenario 1

4.5 Simulation results and discussions

4.5.1 Scenario 1

Figure 12 shows the actual queue length of the buffer in the IP router. We observe that the queue length with threshold-based wavelength allocation method and biologically-inspired wavelength allocation method is less than that with the fixed wavelength allocation method (Fig 12(a)) . The queue length with the optimal wavelength allocation (Fig 12(a)) is less than the biologically-inspired wavelength allocation method, but the difference is marginal. To see how four wavelength allocation methods work, we show the time variation of bandwidth allocated for the packet switching plane in Figure 13. Both the threshold-based wavelength allocation method (Figure 13(c)) and the biologically-inspired wavelength allocation method (Figure 13(d)) adaptively changes

(a) Optimal wavelength allocation

(b) Fixed wavelength allocation

(c) Threshold-based wavelength allocation

(d) Biologically-inspired wavelength allocation
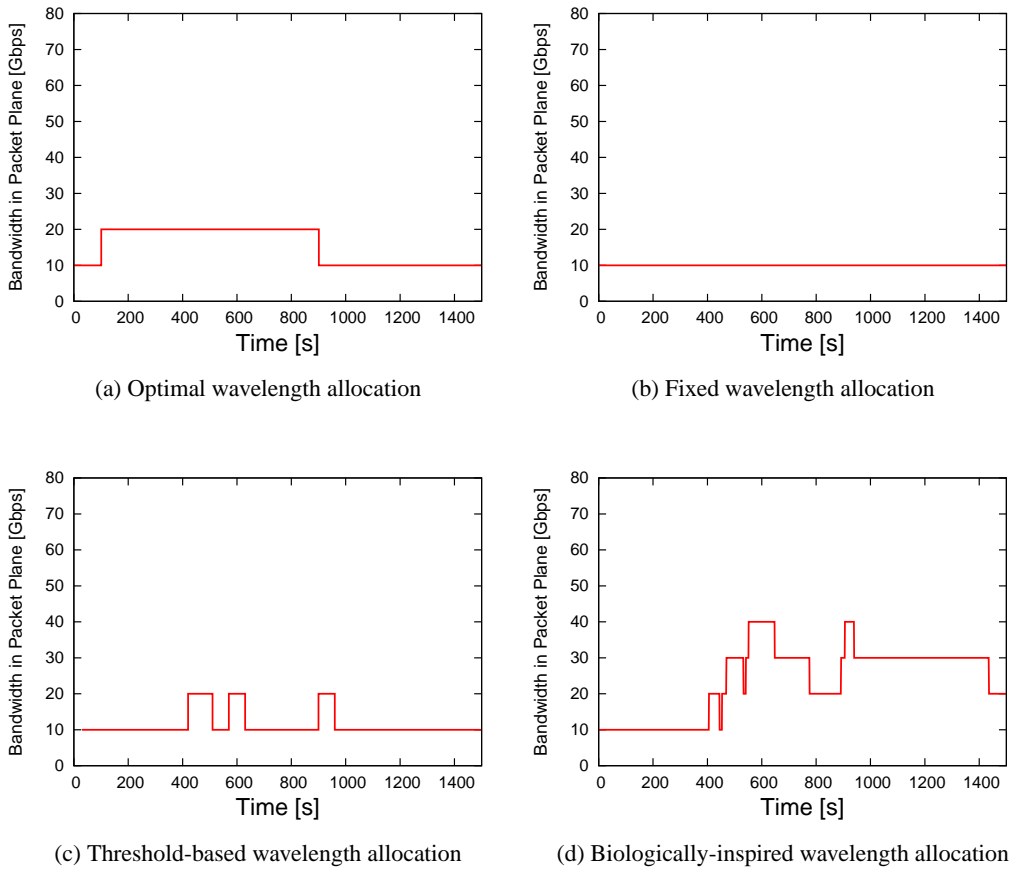
Figure 13: Time variation of the bandwidth in the packet switching plane : Scenario 1

the bandwidth for the packet switching plane. The bandwidth allocation of biologically-inspired wavelength allocation is close to the optimal wavelength allocation. Figure 14 shows the latency of TCP connections that are transferred through the packet switching plane. X-axis represents the time when a TCP connection finishes and Y-axis represent the latency of the TCP connection. Since the threshold-based and biologically-inspired wavelength allocation method decreases the average queue length during the higher arrival rate, the latency of TCP connection is greatly reduced, which in turn decreases the average latency in the path/packet integrated networks. Figure 15 shows the accumulated packet loss for each wavelength allocation method. Note that no packet loss occurs in the case of the optimal wavelength allocation. The biologically-inspired wavelength allocation method takes the second smallest number of packet loss.

We next investigate the biologically-inspired wavelength allocation method in detail. To un-

27

(a) Optimal wavelength allocation

(b) Fixed wavelength allocation

(c) Threshold-based wavelength allocation

(d) Biologically-inspired wavelength allocation
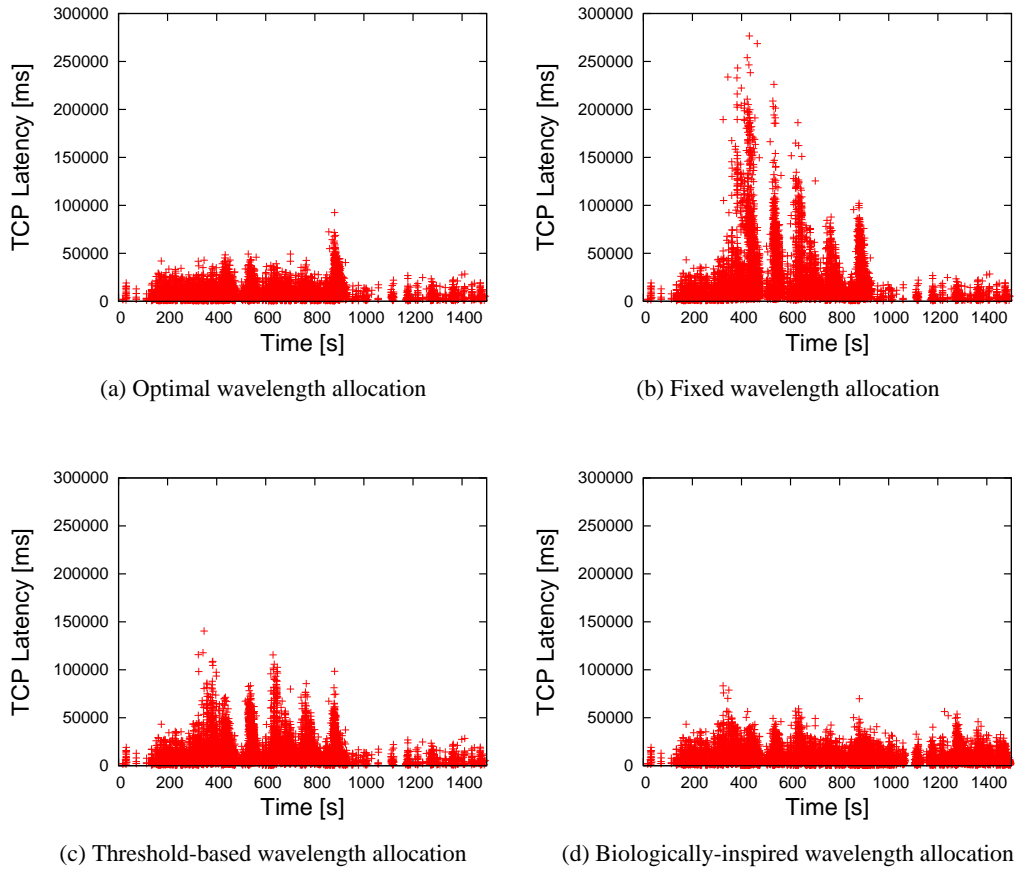
Figure 14: Latency of TCP connections : Scenario 1

derstand the behaviors of biologically-inspired wavelength allocation method, we show the time variation of number of bacteria in Figure 16(a) and the conversion rate in Figure 16(b). We observe that when the conversion rate in the packet switching plane is drastically decreased, the number of bacteria that corresponds to the path switching plane is drastically increased. This is because the biological symbiosis model allocates the wavelength resources effectively when the traffic load on the path switching plane and the packet switching plane is not balanced. Table 4 shows the overall latency in path/packet integrated networks and the latency of data transfers that uses the packet switching plane. Note that when the lightpath establishment succeeds, the latency is around 180 [ms] since the data itransfer time with the bandwidth of lightpath. From Table 4, we observe that the biologically-inspired wavelength allocation method makes the latency to be low.
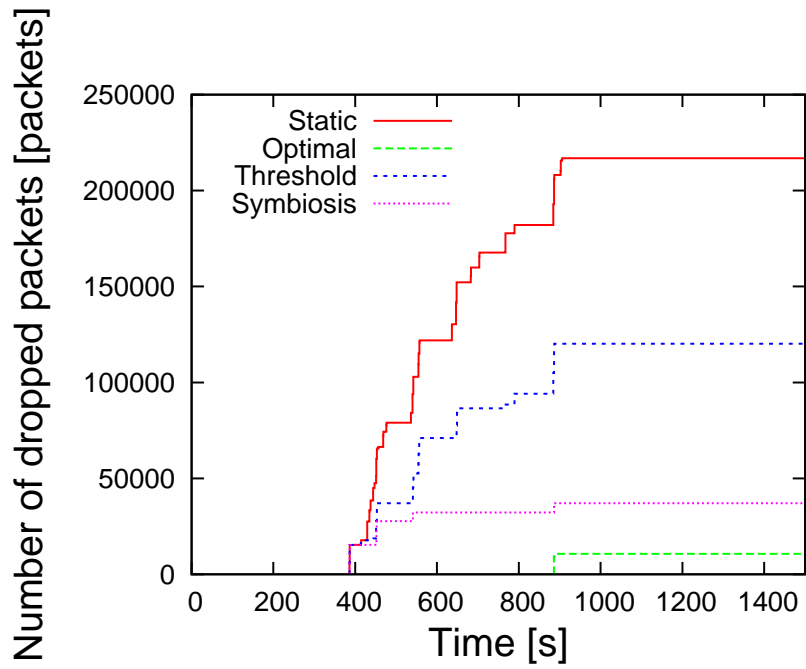
Figure 15: Accumulated packet loss : Scenario 1

Table 4: Simulation results for threshold-based wavelength allocation methods : Scenario 1

	Fixed	Threshold-based	Biologically-inspired	Optimal
Latency (overall)	6407 [ms]	3645 [ms]	2577 [ms]	2409 [ms]
Latency (packet switching plane)	25133 [ms]	14979 [ms]	9480 [ms]	8871 [ms]
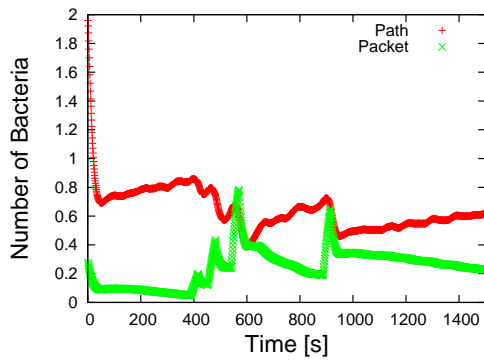
(a) Time variation of number of bacteria
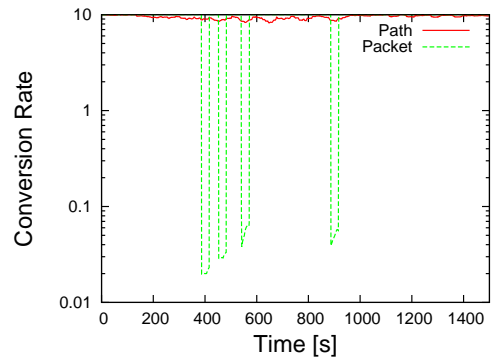
(b) Time variation of conversion rate

Figure 16: Behavior of biological symbiosis model : Scenario 1

29

(a) Optimal wavelength allocation

(b) Fixed wavelength allocation

(c) Threshold-based wavelength allocation

(d) Biologically-inspired wavelength allocation
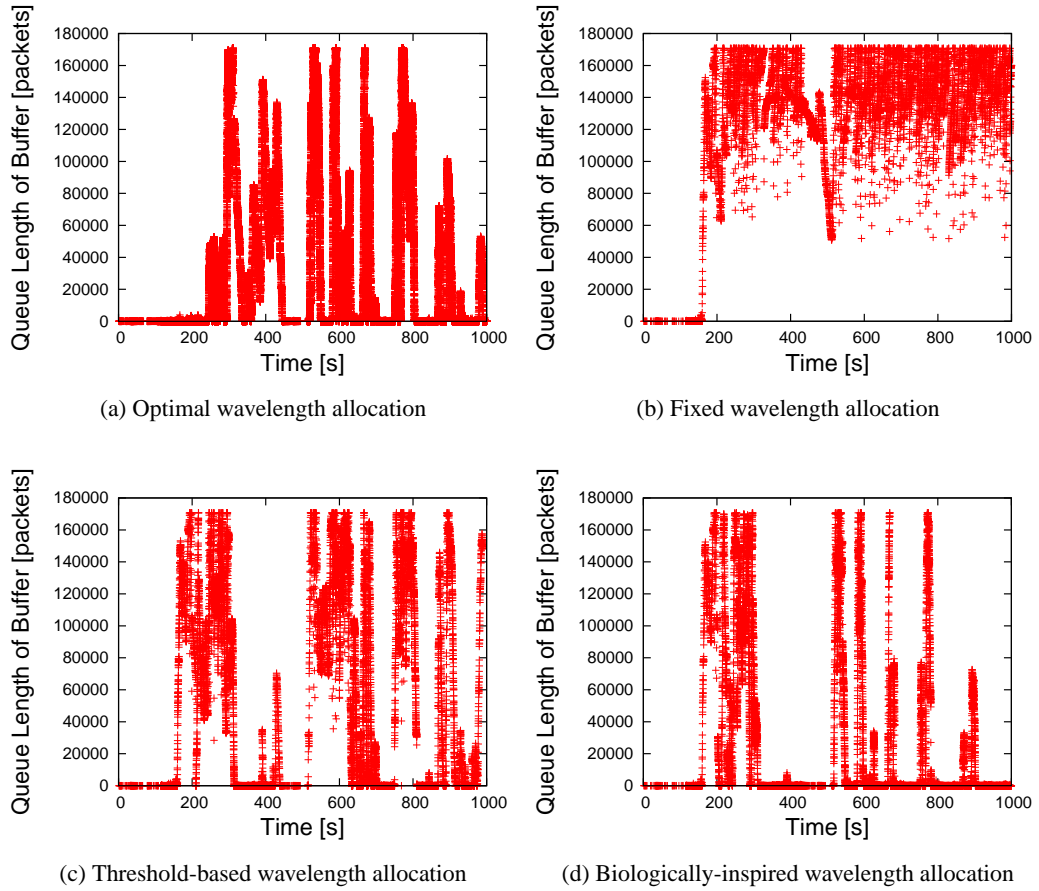
Figure 17: Time variation of queue length : scenario 2

4.5.2 Scenario 2

The arrival rate used in Scenario 2 is shown in Figure 11(b). We also show the results for time-variation of queue length (Figure 17), bandwidth allocated for the packet switching plane (Figure 18), latency of TCP connections (Figure 19), and accumulated packet loss (Figure 20). The simulation results of Scenario 2 are almost the same as the simulation results of Scenario 1; the biologically-inspired wavelength allocation method makes latency low. Against the changes of arrival rate, the biological symbiosis model adaptively changes the number of bacteria (Figure 21). These results show that the biologically-inspired wavelength allocation model achieves adaptive wavelength allocation against the changes of network environments.

(a) Optimal wavelength allocation

(b) Fixed wavelength allocation

(c) Threshold-based wavelength allocation

(d) Biologically-inspired wavelength allocation
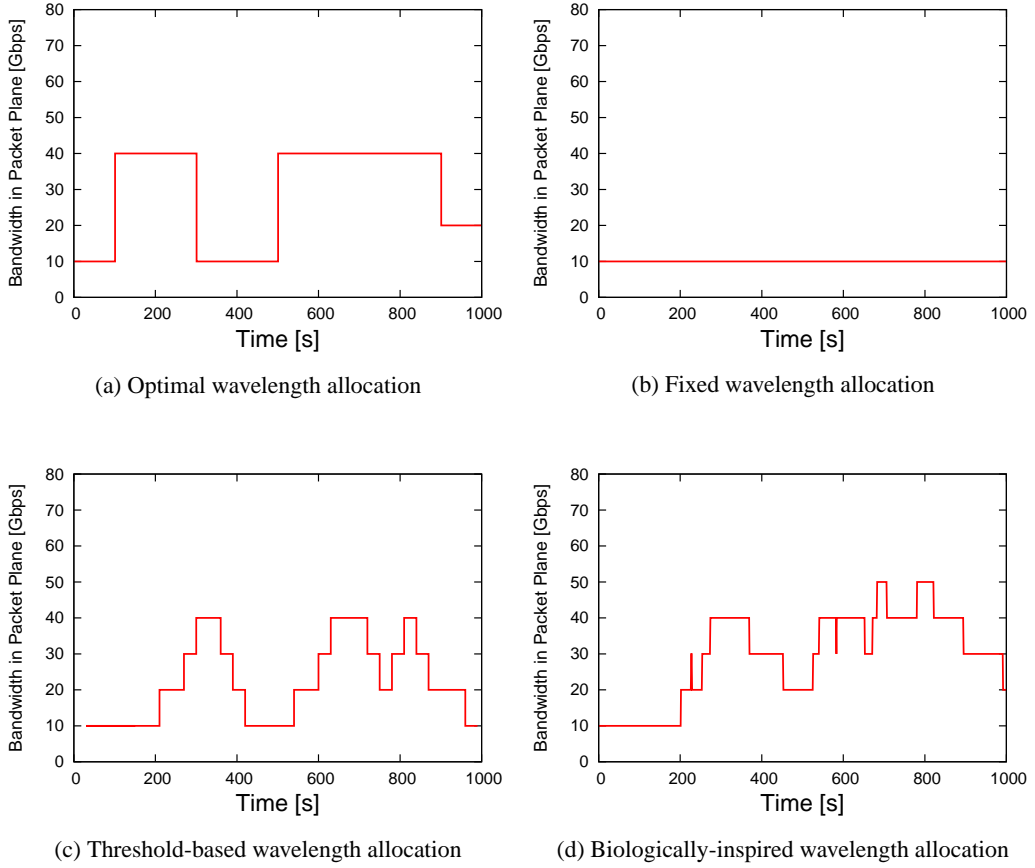
Figure 18: Time variation of the bandwidth in the packet switching plane : Scenario 2

Table 5: Simulation results for threshold-based wavelength allocation methods : Scenario 2

	Fixed	Threshold-based	Biologically-inspired	Optimal
Latency (overall)	14731 [ms]	7462 [ms]	4789 [ms]	5132 [ms]
Latency (packet switching plane)	53856 [ms]	16723 [ms]	9974 [ms]	9715 [ms]

(a) Optimal wavelength allocation

(b) Fixed wavelength allocation

(c) Threshold-based wavelength allocation

(d) Biologically-inspired wavelength allocation
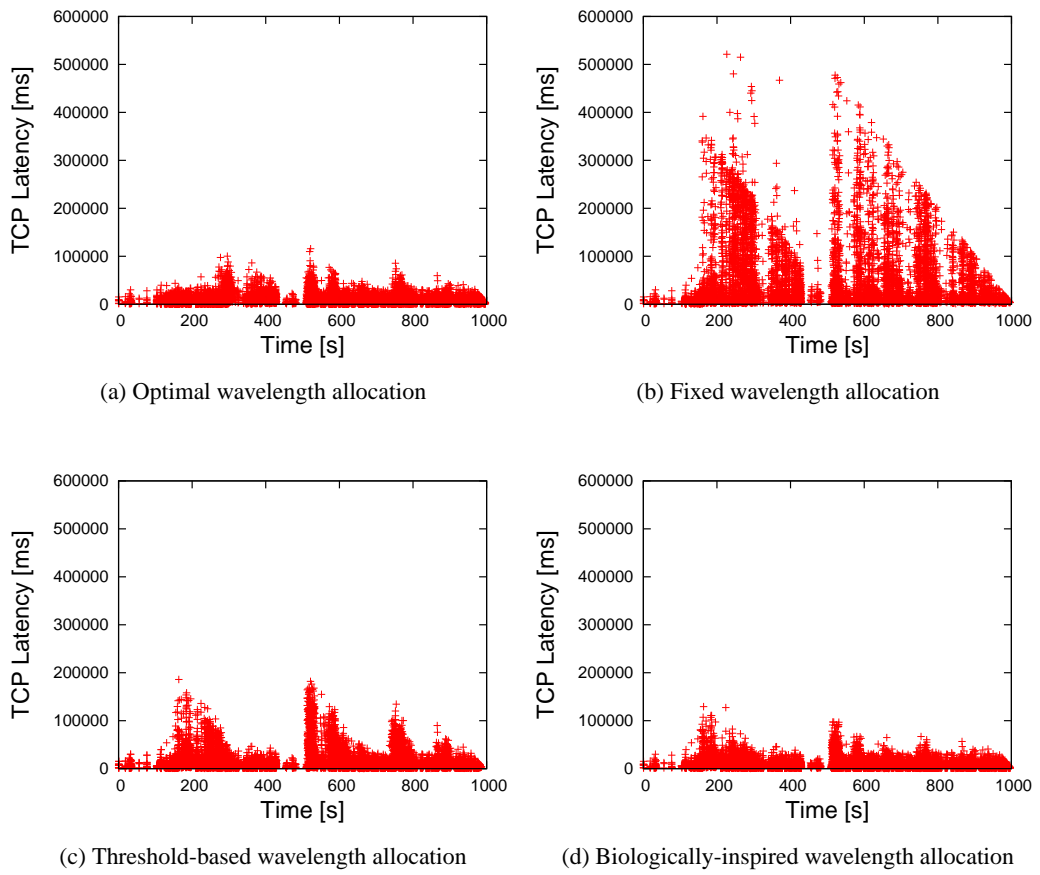
Figure 19: Latency of TCP connections : Scenario 2

32
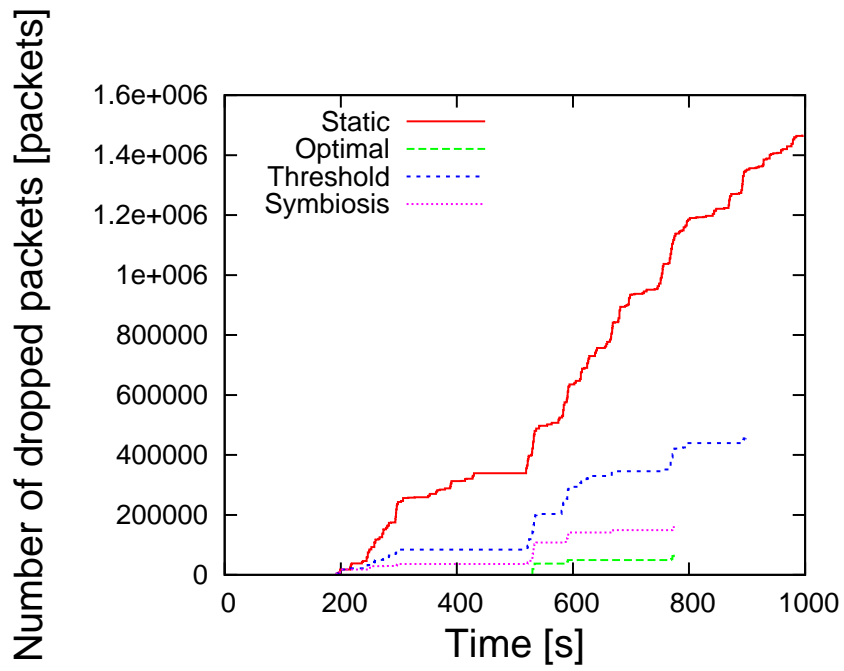
Figure 20: Accumulated packet loss : Scenario 2

(a) Time variation of number of bacteria

(b) Time variation of conversion rate
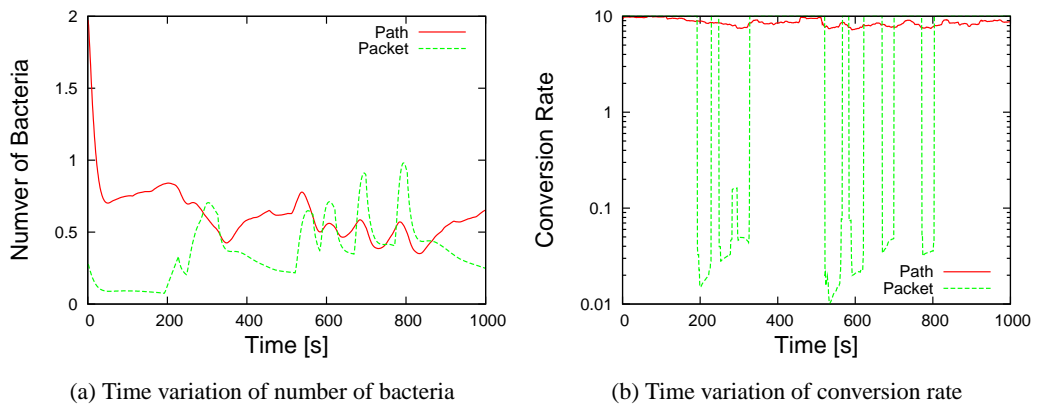
Figure 21: Behavior of biological symbiosis model : Scenario 2

(a) Optimal wavelength allocation

(b) Fixed wavelength allocation

(c) Threshold-based wavelength allocation

(d) Biologically-inspired wavelength allocation
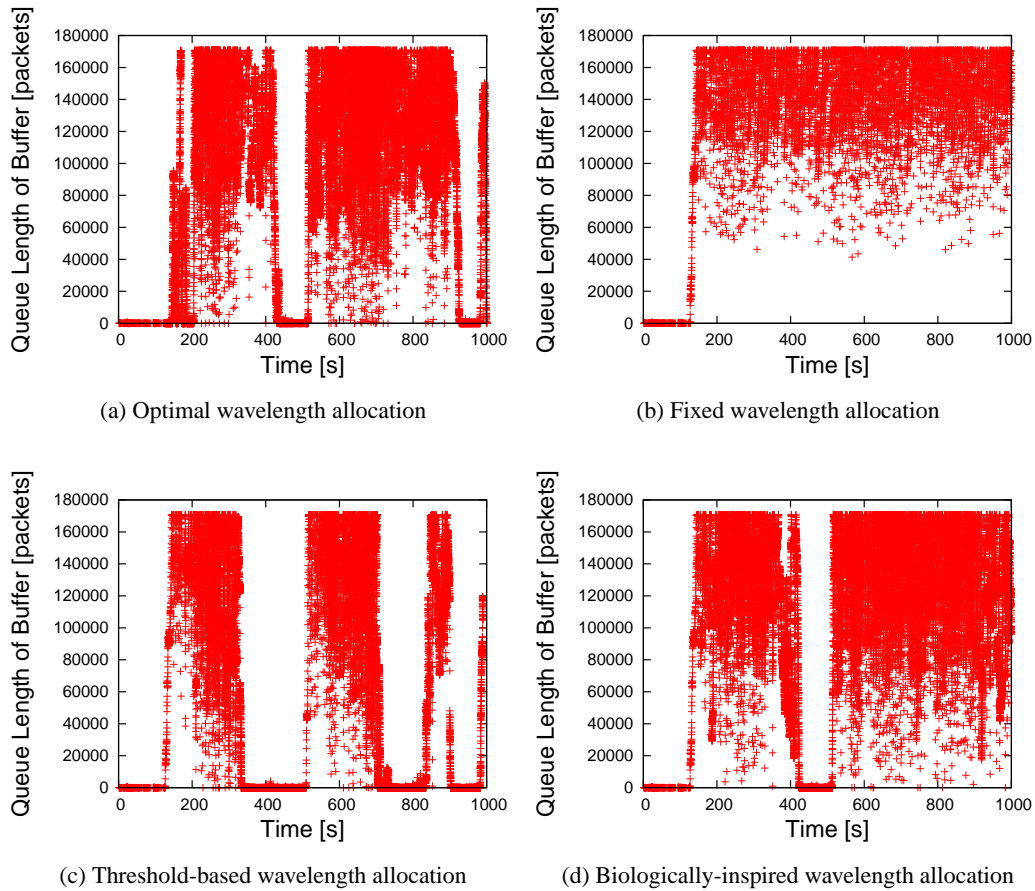
Figure 22: Time variation of queue length : Scenario 3

4.5.3 Scenario 3

The arrival rate used in Scenario 3 is shown in Figure 11(c). The traffic load is much higher than that of Scenario 2. Figure 22 shows the time-variation of queue length. Looking at Figure 22(c), the queue length sharply decreases during [320s- 500s] and [700s-800s]. This is because the traffic load is extremely heavy and threshold-based wavelength allocation method continues to increase the amount of wavelengths allocated to the packet switching plane (See Figure 23). However, the biologically-inspired wavelength allocation method fails to adapt the environmental changes. The main reason for this is amount of wavelengths allocated to the packet switching plane in this simulation is limited by the biological symbiosis model. In summary, the biologically-inspired wavelength allocation method can adapt the changes of network environment efficiently. However, at the extremely high traffic load, the overall latency is mostly the same as the threshold-based

34

(a) Optimal wavelength allocation

(b) Fixed wavelength allocation

(c) Threshold-based wavelength allocation

(d) Biologically-inspired wavelength allocation
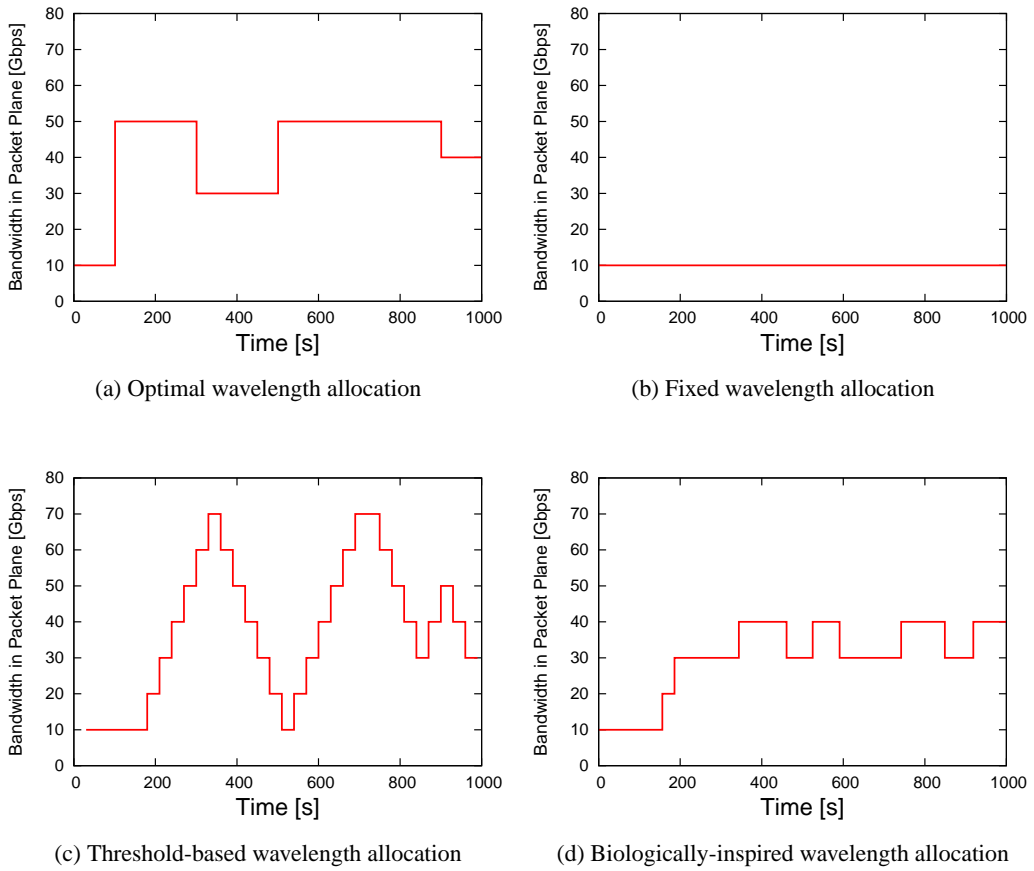
Figure 23: Time variation of the bandwidth in the packet switching plane : Scenario 3

wavelength allocation method. We believe the parameter setting will resolve the problem, but it is left for one of our future works.

5 Conclusions

We evaluated the performance of path/packet integrated networks via computer simulations with respect to the latency. We first observed that the optimal number of wavelengths allocated to the packet switching plane and the path switching plane on various traffic load. We therefore developed two dynamic wavelength allocation methods to decrease the latency on various traffic load. Simulation results show dynamic wavelength allocation methods reduce the latency more than 50% from the fixed wavelength allocation. The results also show that biologically-inspired

(a) Optimal wavelength allocation

(b) Fixed wavelength allocation

(c) Threshold-based wavelength allocation

(d) Biologically-inspired wavelength allocation
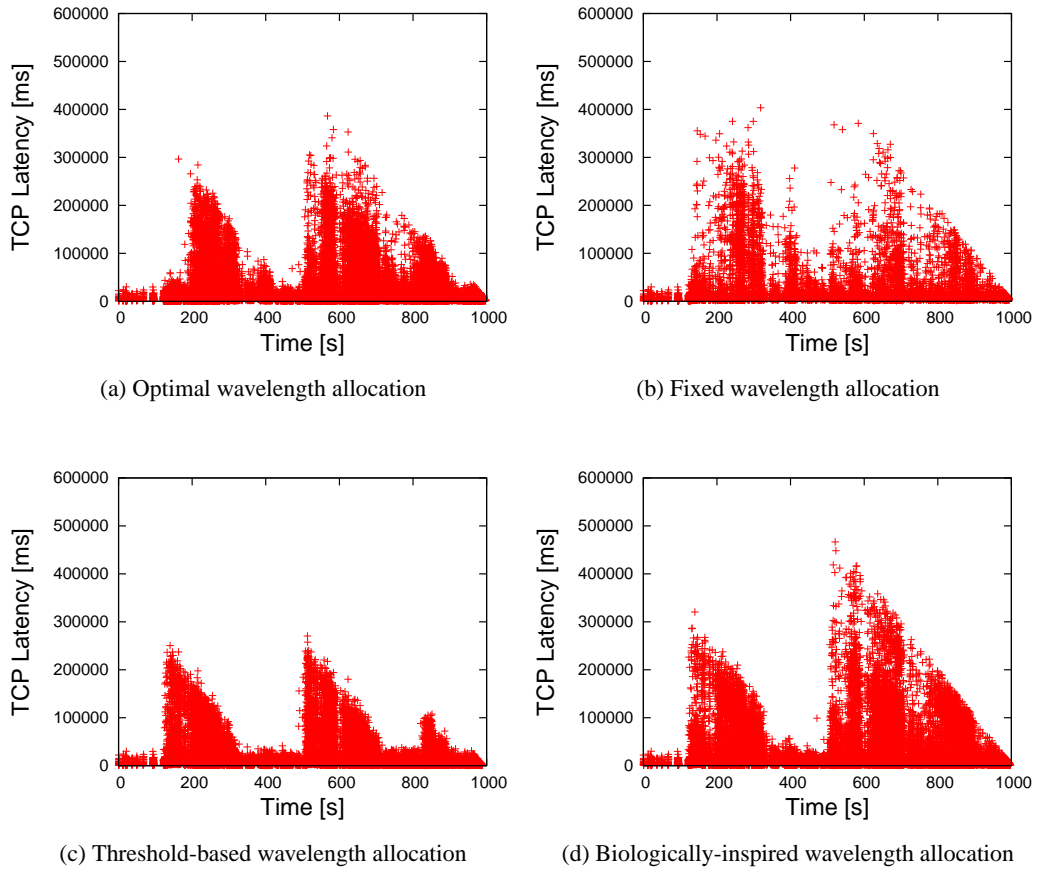
Figure 24: Latency of TCP connections : Scenario 3

wavelength allocation method achieves a nealy 40% reduction from threshold-based wavelength allocation method. Our future work is to develop an OPS/OCS integrated architecture and to evaluate the performance by using the biologically-inspired wavelength allocation method.
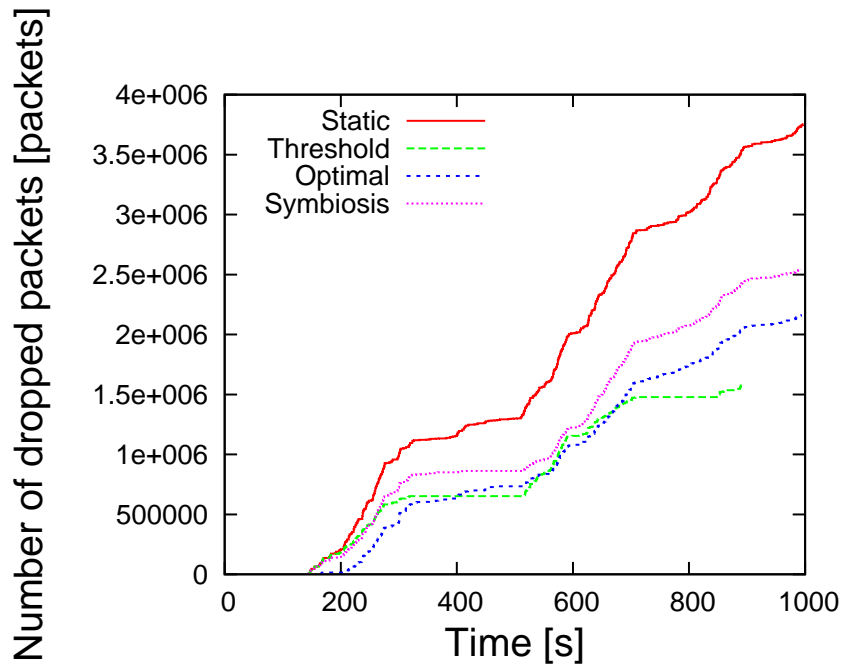
Figure 25: Accumulated packet loss : Scenario 3

Table 6: Simulation results for threshold-based wavelength allocation methods : Scenario 3

	Fixed	Threshold-based	Biologically-inspired	Optimal
Latency (overall)	8922 [ms]	14442 [ms]	22534 [ms]	18776 [ms]
Latency (packet switching plane)	35866 [ms]	27549 [ms]	39464 [ms]	26752 [ms]
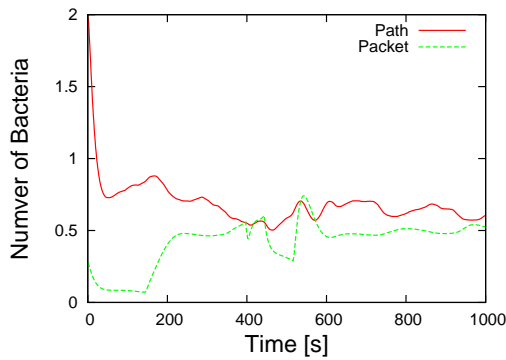
(a) Time variation of number of bacteria
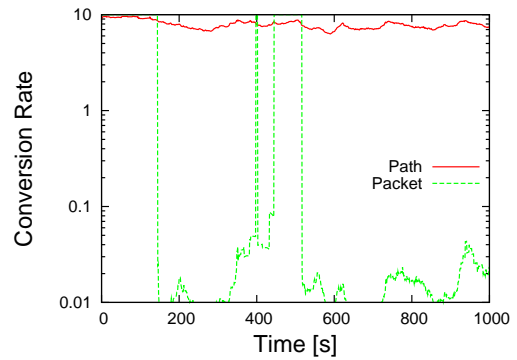
(b) Time variation of conversion rate

Figure 26: Behavior of biological symbiosis model : Scenario 3

37

Acknowledgement

References

[1] K. G. Coffman and A. M. Odlyzko, "Internet growth: Is there a "Moore's Law" for data traffic?." http://www.research.att.com/ amo/doc/internet.moore.pdf.

[2] K.H.Liu, *IP over WDM*. John Wiley & Sons Inc, November 2002. ISBN:0-470-84417-5.

[3] H. Zang, J. P.Jue, L. Sahasrabuddhe, R. Ramamurthy, and B. Mukherjee, "Dynamic light-path establishment in wavelength-routed WDM networks," *IEEE Communications Magazine*, pp. 100–108, Sept. 2001.

[4] M. Veeraraghavan, X. Zheng, W. Feng, H. Lee, E. K. Chong, and H. Li, "Scheduling and transport for file transfers on high-speed optical circuits," *Journal of Grid Computing*, vol. 1, pp. 395–405, Dec. 2003.

[5] M. Kodialanm and T. V. Lakshman, "Intergrated dynamic IP and wavelength routing in IP over WDM networks," in *Proceedings of IEEE INFOCOM*, pp. 358–366, Apr. 2001.

[6] R. Ramaswami and K. N. Sivarajan, "Design of logical topologies for wavelength-routed optical networks," *IEEE Journal on Selected Areas in Communications*, vol. 14, pp. 840–851, June 1996.

[7] S. Lin and N. McKeown, "A simulation study of IP switching," in *Proceedings of ACM SIGMCOM1997*, pp. 15–24, Sept. 1997.

[8] M. Ohashi, S. Arakawa, and M. Murata, "Implementation and evaluation of fast lightpath setup method in wavelength-routed WDM networks," in *Proceedings of SPIE APOC 2006*, vol. 6354, pp. 63541V–1 – 63541V–9, Sept. 2006.

[9] T. Yomo, W.-Z. Xu, and I. Urabe, "Mathematical model allowing the coexistence of closely related competitors at the initial stage of evolution," *Researched on Population Elocogy*, vol. 38, no. 2, pp. 239–247, 1996.

[10] H. Jiang and C. Dovrolis, "Passive estimation of TCP round-trip times," *ACM SIGCOMM Computer Communication Review*, vol. 32, pp. 75–88, July 2002.